ChemComm
Chemical Communications

This article can be cited before page numbers have been issued, to do this please use: Q. Yu, H. Su, G. Zhai, S. Zhang, L. Sun, J. Chen and X. Li, *Chem. Commun.*, 2020, DOI: 10.1039/D0CC06764D.

ROYAL SOCIETY OF CHEMISTRY

rsc.li/chemcomm

View Article Online
DOI: 10.1039/D0CC06764D

COMMUNICATION

Designed Electron-Deficient Gold Nanoparticles for Room-Temperature C_{sp3}-C_{sp3} Coupling Reaction

Qiu-Ying Yu, Hui Su, Guang-Yao Zhai, Shi-Nan Zhang, Lu-Han Sun, Jie-Sheng Chen and Xin-Hao Li*

Received 00th January 20xx,
Accepted 00th January 20xx

DOI: 10.1039/x0xx00000x

Stille cross-coupling reactions catalysed by an ideal catalyst combining the high activity of homogeneous catalysts and the reusability of heterogeneous catalysts are of great interest for C-C bond formation, which is a widely used reaction in fine chemistry. Despite great effort to increase the utilization ratio of surface metal atoms, the activity of heterogeneous catalysts under mild conditions remains unsatisfactory. Herein, we design a proof-of-concept strategy to trigger the room-temperature activity of heterogeneous Au catalysts by decreasing the electron density at the interface of a rationally designed Schottky heterojunction of Au metals and boron-doped carbons. The electron-deficient Au nanoparticles formed as a result of the rectifying contact with boron-doped carbons facilitate the autocleavage of C-Br bonds for highly efficient C-C coupling reactions of alkylbromides and allylstannanes with a TOF value of 5199 h^{-1} at room temperature, surpassing that of the state-of-art homogeneous catalyst .

The noble metal-catalysed Stille cross-coupling reaction is an efficient approaches for the chemical synthesis of C-C bonds.[1-2] Despite great effort in the development of homogeneous catalysts,[3] the activity of noble metal nanocatalysts in C-C bond formation reactions is far from satisfactory.[2,4-6] There is a consensus in the literature that the application of supported noble metal nanoparticles usually requires harsh reaction conditions accompanied by unwanted degradation of the substrates or products.[5,7-8] The relatively low utilization ratio of the surface atoms of noble metal nanoparticles further decreases their turnover frequencies compared to the those of homogeneous systems.[5]

The support effect is a powerful and straightforward means to increase the activity of embedded metal nanoparticles.[9-12] Even though carbon-supported noble metal nanoparticles (e.g., Pd/C, Pt/C) have been widely used as reusable catalysts for various coupling reactions,[13] taking advantage of the synergy between metal nanoparticles and a support to make the heterogeneous catalysts more active than their homogeneous counterparts has never been achieved for mild carbon-carbon coupling reactions until now.[14-15]

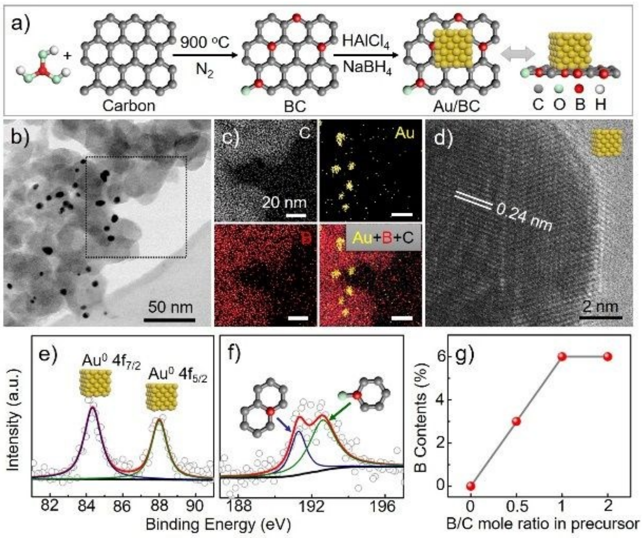

Fig. 1 Synthesis and structures of Au/BC samples. (a) Formation and structure of BC-x and Au/BC. TEM (b), EDX elemental mapping (c) and HRTEM (d) images of a typical $Au_{0.1}$/BC-1 sample. Au 4f (e) and B 1s (f) XPS spectra of a typical $Au_{0.1}$/BC-1 sample. (g) The B content in $Au_{0.1}$/BC-x estimated by inductively coupled plasma optical emission spectrometry (ICP-OES) analysis.

Herein, we report a conceptually new strategy to boost the room-temperature activation of alkylbromides on metallic gold nanoparticles via the rectifying contact with boron-doped carbons (Au/BC), resulting in catalytic activity for Stille coupling with allylstannanes greater than that of homogeneous materials. Theoretical simulations, which were validated by experimental results, predict that the Schottky heterojunction significantly increases the automatic electron flow from Au to BC with an even lower work function, allowing the room-temperature activation of alkylbromides and subsequent formation of C-C bonds. We also tune the electron density of Au by rational control of the boron content, and this method is a powerful tool to directly optimize the activity of supported

---

School of Chemistry and Chemical Engineering, Shanghai Jiao Tong University, Shanghai 200240, P. R. China.
Electronic Supplementary Information (ESI) available: See DOI: 10.1039/x0xx00000x

electron-deficient Au nanoparticles, resulting in a turnover frequency (TOF) of 17329 h^{-1} at 50 °C, a value not only far surpassing the TOF of the state-of-the-art heterogeneous nanocatalyst but also even higher than that of reported homogeneous catalysts under similar reaction conditions.[8,16-17] The optimized Au/BC catalyst also exhibits unexpected room-temperature activity for C-C Stille coupling.

With respect to the on-demand design of effective centres, electron-deficient metals might be preferred for specific reactions (as exemplified by the activation of alkylbromides in this work). Due to the relatively high work functions of noble metals, most noble metals tend to accept electrons from various catalyst supports, including "noble" carbons with various nitrogen dopants as a typical example.[18-21] However, exploration of possible support materials that could attract electrons and tune the activity of noble metals has been less studied until now. We thus focus on the design of electron-deficient carbon supports by introducing boron dopants as electron acceptors to largely pull down the valence band of carbon.[22] As shown in Figure 1a, the mixture of boric acid and activated carbon was condensed at 900 °C to obtain boron-doped carbons (BC-x), where x (0-2) indicates the molar ratio of B and carbon species. Gold nanoparticles were further deposited via a modified wet impregnation method to obtain Au_y/BC-x samples (y: weight percentages of Au in Au_y/BC-x).

Au nanoparticles with a mean size of 6 nm were deposited on the carbon support, as demonstrated by scanning electron microscopy (SEM) and transmission electron microscopy (TEM) observations (Figure 1b and Figure S1-S2). The energy dispersive X-ray spectroscopy (EDX) elemental mapping images further indicated the uniform distribution of boron elements and Au nanoparticles along the carbon support (Figure 1c). The high-resolution TEM (HRTEM) image of $Au_{0.1}$/BC-1 exhibited typical lattice fringes of 0.24 nm, attributed to the (111) planes of metallic Au (Figure 1d),[23] which was also confirmed by the typical X-ray photoemission spectroscopy (XPS) peaks (Figure 1e) and X-ray diffraction (XRD) peaks (Figure S3) of metallic Au in the $Au_{0.1}$/BC-1 sample.

More importantly, the content of B dopants in typical $Au_{0.1}$/BC samples, mainly within B-C and C-B-O bonds (Figure 1f), could be gradually enriched from 0 to 6% simply by adding more boric acid to the solid precursor (Figure 1g and Table S1). It should be noted that the addition of an excess amount of boric acid could not further elevate the concentration of B dopants (Figure 1g and Figure S4), presumably due to the diffusion limitation for the solid-state reaction between boric acid and carbon spheres. Such a reaction also leads to the deconstruction of carbon spheres and thus a slight decrease in the pore volume and surface area of $Au_{0.1}$/BC-2 (Figure S5, Table S2).

The strong interaction between B-doped carbon and Au nanoparticles was well reflected by the interfacial electron exchange. The density functional theory (DFT) simulation results (Figure 2a and Figure S6) directly indicate the electron density difference (EDD) of Au nanoparticles with more electrons (0.14 electrons per Au atom) flowing to the boron-doped carbon support than are flowing to the pristine carbon (-0.0018 electrons per Au atom). Such a rectifying contact between Au and boron-doped carbons was then validated experimentally via careful analysis of the electronic structures of heterojunctions. The Mott-Schottky plots (Figure S7) and current-voltage curves (Figure S8) of carbon supports show the band structures of these materials, with the valence bands largely pulled down due to the increased boron concentration; moreover, the bandgap was also gradually enlarged from pristine carbon to BC-0.5 to BC-1 (Figure 2b). It is thus possible that boron-rich carbon supports with lower work functions attract more electrons from Au nanoparticles via the interfacial Schottky effect (Figure 2b right).[9-12] Indeed, the XPS Au peaks gradually shifted to higher binding energy as the boron concentration in the carbon supports increased (Figure 2c and Figures S9), confirming the enhanced electron deficiency of embedded Au nanoparticles, which was also confirmed by the increased work functions (Figure 2d) of the Au nanoparticles that were estimated via ultraviolet photoelectron spectroscopy (UPS) analysis (Figures S10).

View Article Online
DOI: 10.1039/D0CC06764D

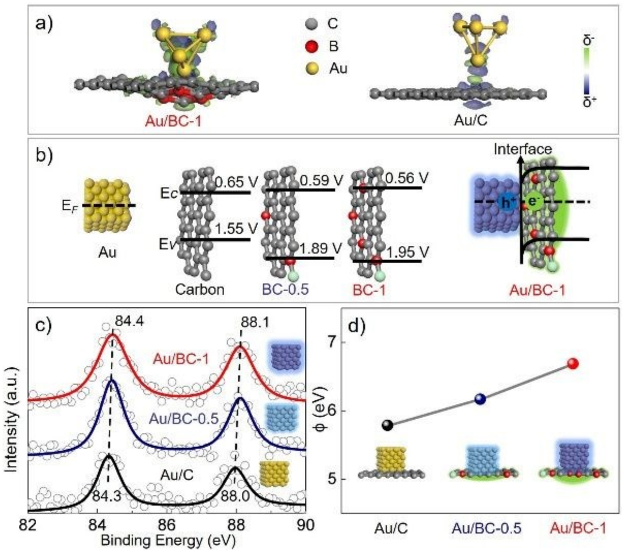

Fig. 2 Electron deficiency of Au nanoparticles in Au/BC samples. (a) EDD stereograms of Au/BC-1 and Au/C models. (b) The work functions of Au and band structures of BC-1, BC-0.5 and carbon support obtained from Mott-Schottky plots and current-voltage curve (left). Scheme of the Mott-Schottky rectifying contact between Au nanoparticles and boron-doped carbon support, resulting in electron-deficient (blue) and electron-rich (green) areas (right). The Au 4f XPS spectra (c) and calculated work functions (d) from the UPS results of Au/BC-1, Au/BC-0.5 and Au/C catalysts.

The success in tuning the electron deficiency of gold nanoparticles prompted us to test the possible catalytic activity of these materials for the Stille coupling of (1-bromoethyl) benzene and allyltributylstannane as a model reaction under mild conditions (Figure 3a and Table S3). The model reaction did not proceed without a catalyst or when bare boron-doped carbons (e.g., BC-1) were used as the catalyst. Au/C without B dopants resulted in moderate conversion (33%) of the same substrates at 50 °C. Surprisingly, the Au/BC-1 sample containing electron-deficient Au nanoparticles resulted in complete

View Article Online
DOI: 10.1039/D0CC06764D

conversion of the substrate under fixed conditions, even though the sizes and weight ratios (Table S1) of the Au nanoparticles were similar to those of the Au/C catalyst. The hot-filtration test (hollow spheres in Figure 3a) directly excluded the obvious contribution of soluble Au components to the catalytic activity. All these results indicate the key role of Au nanoparticles as active sites for this coupling reaction. The heterogeneous nature of the Au/BC catalyst was further confirmed by its excellent reusability (Figure 3b and Table S4). The recycled catalyst can be used for at least four successive cycles of reactions with fixed selectivity (> 99%) and only a slight loss of conversion due to the loss of catalyst during the separation process via centrifugation and washing. Both the structure and the composition (Figure S11) of the Au/BC-1 catalyst remain nearly the same after use.

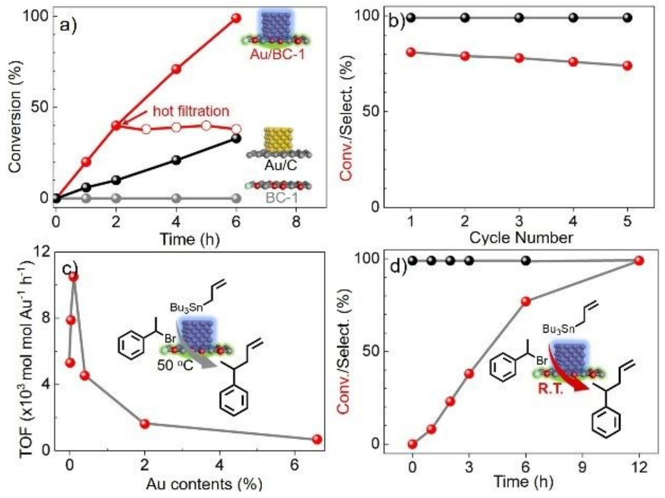

Fig. 3 Stille cross-coupling reaction over electron-deficient Au nanoparticles. (a) Conversions of the coupling reaction over Au/BC-1, Au/C and BC-1 at different times. Hot filtration test over a typical Au/BC-1 catalyst (hollow spheres). (b) Conversions and selectivity of the coupling reaction over Au/BC-1 during four cycles. (c) TOF values of catalysts with different Au contents. (d) Conversions and selectivity of the coupling reaction over Au/BC-1 at different times at room temperature. Reaction conditions: 1.2 mmol of (1-bromoethyl) benzene, 3 mmol of allyltributylstannane, 10 mg of catalyst for (a), (b) and (d); 3 mg of catalyst for (c); 50 °C or room temperature for 1 h (c) or 5 h (b).

The catalytic activity of electron-deficient Au nanoparticles can be optimized by adjusting the weight ratios of Au nanoparticles and boron-doped carbons (Figure 3c and Table S5), demonstrating the synergistic effect of the two components on facilitating the coupling reaction. As the best catalyst in this work, the Au/BC-1 catalyst with a Au content of 0.1% was used for subsequent reactions and characterizations without any modification. Most importantly, the room-temperature coupling of (1-bromoethyl) benzene and allyltributylstannane proceeded smoothly on the Au/BC-1 catalyst under ambient conditions (Figure 3d) and achieved complete conversion within 12 h. Such a room-temperature activity of Au/BC-1 with excellent chemical tolerance of substituted benzylic bromides and allylstannanes (Figure S12) is preferred for the production of less stable substrates or products that are susceptible to thermal degradation.

To determine the origin of the room-temperature activity of electron-deficient Au nanocatalysts for C-Br activation, we investigated the adsorption and activation of (1-bromoethyl) benzene as the model molecule on the Au surface via both theoretical and experimental methods. The calculated adsorption energy (ΔE_{ads}) of (1-bromoethyl) benzene on electron-deficient Au in the Au/BC model (-0.30 eV) is slightly higher than that in the Au/C model (-0.28 eV) (Figure 4a). More importantly, the equilibrium distance between the surface of electron-deficient Au and the adjacent Br of (1-bromoethyl) benzene is only 2.3 Å, directly indicating preferred adsorption of the C-Br bond to the Au surface of the Au/BC model (Figure 4b).[24-25] The temperature-programmed desorption (TPD) analysis results exhibit a new strong adsorption peak for (1-bromoethyl) benzene over the Au/BC catalysts (Figure 4c) at a lower temperature than that of the Au/C catalyst. The fact that the bare BC-1 support results in negligible adsorption of the (1-bromoethyl) benzene molecules directly demonstrates the key role of the electron-deficient Au in enhancing the preadsorption of the (1-bromoethyl) benzene, benefiting the subsequent activation process of the C-Br bond for coupling with highly active allylstannanes.

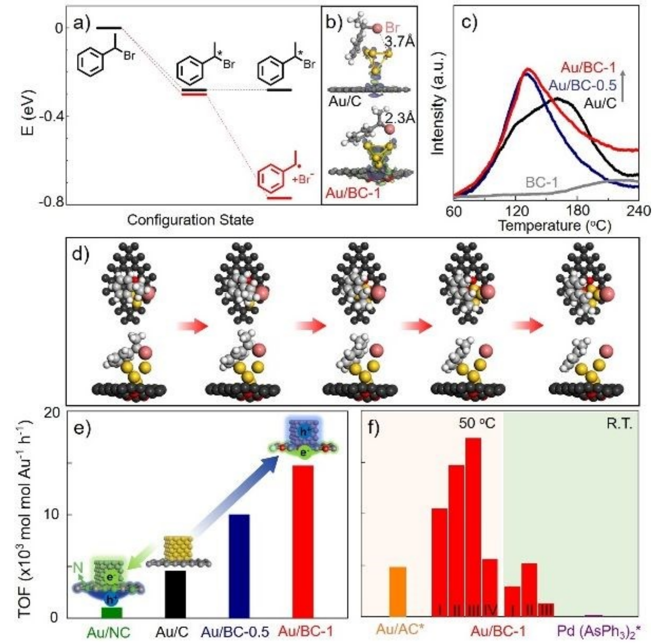

Fig. 4 Effect of the electron deficiency of Au nanoparticles on the Stille coupling reaction. Calculated energy during the adsorption of (1-bromoethyl) benzene to Au/BC-1 (red) and Au/C (black) catalysts (a) and the corresponding configurations (b). (c) The (1-bromoethyl) benzene-TPD analysis of the Au/BC-1, Au/BC-0.5, Au/C and BC-1 samples. (d) The calculated configurations of the Au/BC-1 model during the activation of the C-Br bond in (1-bromoethyl) benzene (top view and side view). (e) TOF values of the Au/BC-1, Au/BC-0.5, Au/C and Au/NC catalysts. Reaction conditions: 47.5 mmol of (1-bromoethyl) benzene, 57 mmol of allyltributylstannane, 12 mg of catalyst, 50 °C, 6 h. (f) TOF values of the latest reported Au catalyst deposited on active carbons (AC) and homogeneous Pd catalyst in the

literature and our Au/BC-1 catalyst at different temperatures. (Au mol %: I 0.00076, II 0.000077, III 0.000038, IV 0.000026.)

Cleavage of the C-Br bonds of preadsorbed (1-bromoethyl) benzene on Au/BC-1 is exothermic by 0.47 eV (Figure 4a). Unlike the unchanged configuration of (1-bromoethyl) benzene on Au/C, the calculated configurations of (1-bromoethyl) benzene on the electron-deficient Au of Au/BC-1 exhibit an automatic cleavage of C-Br bonds, resulting in the formation of a benzylic radical and a Br atom adsorbed on the Au surface (Figures 4d and S13, and Supplementary Videos 1-2), indicating a radical pathway for the coupling process, as experimentally validated by the observed homocoupling process (Figure S14). The predicted catalytic mechanism was demonstrated in Figure S15. After determining the dominant effect of electron density on the activity of Au nanoparticles, we were able to experimentally tune the intrinsic activity of Au nanoparticles, as indicated by the TOF values, by changing the type and concentration of dopants (Figure 4e and Table S6). The TOF values for coupling (1-bromoethyl) benzene with allyltributylstannane over Au nanoparticles under fixed reaction conditions could be greatly increased from 4549 h^{-1} to 10026 h^{-1} and then to 14729 h^{-1} for the Au/C, Au/BC-0.5 and Au/BC-1 samples, respectively, with increasing electron deficiency, indicating the adjustable activity of Au nanoparticles along with the increased concentrations of boron dopants. As a control sample, electron-rich Au nanoparticles (Figure S16) embedded in nitrogen-doped carbons provide a TOF value of only 1040 h^{-1} and perform even worse than Au/C, again demonstrating the unique role of electron-deficient Au in activating C-Br bonds for the Stille coupling reaction.

With optimized Au/substrate ratios, the best Au/BC-1 catalyst with the most pronounced electron deficiency exhibited a TOF of 17329 h^{-1} at 50 °C and a remarkably high TOF of 5199 h^{-1} at room temperature (Figures 4f and S17 and Table S7). The TOF value of Au/BC-1 at 50 °C is four times that of the reported Au/AC catalyst. To the best of our knowledge, there is a rather limited number of effective catalysts that could trigger similar reactions at room temperature reported in the literature and confirmed experimentally in this work (Entry 8 in Table S7). The state-of-the-art homogeneous catalyst $Pd(AsPh_3)_2$ exhibited a TOF value of only 30 h^{-1} at room temperature,[26] demonstrating the great potential of heterojunction-based nanocatalysts as highly efficient catalysts for real-life chemical production.

In conclusion, we designed an electron-deficient Au nanoparticle-based catalyst via Schottky contact with boron-doped carbons for room-temperature Stille cross-coupling reactions. The electron deficiency of the Au nanoparticles significantly increased the automatic activation of C-Br bonds in alkylbromides and successive coupling reactions with allylstannanes, surpassing the activity of reported homogeneous catalysts. Tuning the electron density of the Au nanoparticles provided new insights into the design of highly efficient and reusable catalysts for organic synthesis under mild conditions, enhancing the potential of heterogeneous noble metal catalysts to make the manufacture of fine chemicals environmentally friendly.

This work was supported by the National Natural Science Foundation of China (21722103, 21931005, 21720102002, and 21673140), Shanghai Science and Technology Committee (19JC1412600) and the SJTU-MPI partner group.

View Article Online
DOI: 10.1039/D0CC06764D

Conflicts of interest

There are no conflicts to declare.

Notes and references

1 N. Huang, Y. Xu and D. Jiang, *Sci. Rep.*, 2014, **4**, 7228.
2 M. J. Jin and D. H. Lee, *Angew. Chem. Int. Ed.,* 2010, **49**, 1119.
3 C. Cordovilla, C. Bartolomé, J. M. Martínez-Ilarduya and P. Espinet, *ACS Catal.,* 2015, **5**, 3040.
4 A. Ghorbani-Choghamarani and M. Norouzi, *New J. Chem.,* 2016, **40**, 6299.
5 M. Stratakis and H. Garcia, *Chem. Rev.,* 2012, **112**, 4469.
6 T.-N. Ye, Y. Lu, Z. Xiao, J. Li, T. Nakao, H. Abe, Y. Niwa, M. Kitano, T. Tada and H. Hosono, *Nat. Commun.,* 2019, **10**, 5653.
7 M. Pagliaro, V. Pandarus, R. Ciriminna, F. Beland and P. D. Cara, *ChemCatChem,* 2012, **4***,* 432.
8 J. Holz, C. Pfeffer, H. Zuo, D. Beierlein, G. Richter, E. Klemm and R. Peters, *Angew. Chem. Int. Ed.,* 2019, **58**, 10330.
9 Y.-X. Lin, S.-N. Zhang, Z.-H. Xue, J.-J. Zhang, H. Su, T.-J. Zhao, G.-Y. Zhai, X.-H. Li, M. Antonietti and J.-S. Chen, *Nat. Commun.,* 2019, **10**, 4380.
10 Y.-X. Liu, H.-H. Wang, T.-J. Zhao, B. Zhang, H. Su, Z.-H. Xue, X.-H. Li and J.-S. Chen, *J. Am. Chem. Soc.,* 2019, **141**, 38.
11 Z.-H. Xue, J.-T. Han, W.-J. Feng, Q.-Y. Yu, X.-H. Li and J.-S. Chen, *Angew. Chem. Int. Ed.,* 2018, **57**, 2697.
12 H. Su, P. Gao, M.-Y. Wang, G.-Y. Zhai, J.-J. Zhang, T.-J. Zhao, J. Su, M. Antonietti, X.-H. Li and J.-S. Chen, *Angew. Chem. Int. Ed.,* 2018, **57**, 15194.
13 L. Yin and J. Liebscher, *Chem. Rev.,* 2007, **107**, 133.
14 X. Zhang, Z. Sun and B. Wang, *J. Am. Chem. Soc.,* 2018, **140**, 954.
15 Q. Gu, Q. Jia, J. Long and Z. Gao, *ChemCatChem*, 2019, **11**, 669.
16 G. Lu, C. Cai and B. H. Lipshutz, *Green Chem.,* 2013**, 15**, 105.
17 J. C. Garcia-Martinez, R. Lezutekong and R. M. Crooks, *J. Am. Chem. Soc.,* 2005, **127**, 5097.
18 L. He, F. Weniger, H. Neumann and M. Beller, *Angew. Chem. Int. Ed.,* 2016, **55**, 12582.
19 X.-H. Li, M. Baar, S. Blechert and M. Antonietti, *Sci. Rep.,* 2013, **3**, 1743.
20 Z.-H. Xue, S.-N. Zhang, Y.-X. Lin, H. Su, G.-Y. Zhai, J.-T. Han, Q.-Y. Yu, X.-H. Li, M. Antonietti and J.-S. Chen, *J. Am. Chem. Soc.,* 2019, **141**, 14976.
21 X.-H. Li and M. Antonietti, *Chem. Soc. Rev.,* 2013, **42**, 6593.
22 Y. Jia, R. Hu, Q. Zhou, H. Wang, X. Gao and J. Zhang, *J. Catal.,* 2017, **348**, 223.
23 Y. Cai, Y. Guo and J. Liu, *Chem. Commun.,* 2020**, 56**, 876.
24 Z. Chen, E. Vorobyeva, S. Mitchell, E. Fako, M. A. Ortuno, N. Lopez, S. M. Collins, P. A. Midgley, S. Richard, G. Vile and J. Perez-Ramirez, *Nat. Nanotechnol.,* 2018, **13**, 702.
25 T.-N. Ye, S.-W. Park, Y. Lu, J. Li, M. Sasase, M. Kitano, T. Tada and H. Hosono, *Nature,* 2020, **583**, 391.
26 T. O. Ronson, J. R. Carney, A. C. Whitwood, R. J. K. Taylor and J. S. Fairlamb, *Chem. Commun.,* 2015*,* **51**, 3466.

View Article Online
DOI: 10.1039/D0CC06764D

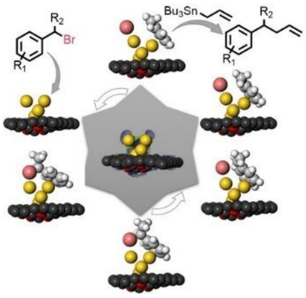

Room-temperature autocleavage of C-Br bonds via electron-deficient Au nanoparticles formed as a result of the rectifying contact with boron-doped carbons.